Reaction of Bulk Protons with a Mitochondrial Inner Membrane Preparation: Time-Resolved Measurements and Their Analysis†

Menachem Gutman,* Alexander B. Kotlyar, Natalia Borovok, and Esther Nachliel

The Laser Laboratory for Fast Reactions in Biology, Department of Biochemistry, The George S. Wise Faculty of Life Sciences, Tel Aviv University, Ramat Aviv 69978, Israel

Received November 25, 1992; Revised Manuscript Received January 19, 1993

ABSTRACT: The laser-induced proton pulse technique [Gutman, M. (1986) *Methods Enzymol. 127*, 522–538] was applied on suspensions of submitochondrial vesicles, and the exchange of protons between the bulk and the mitochondrial membranes was measured in the time-resolved domain with a submicrosecond resolution. The protons were discharged by photoexcitation of pyranine (8-hydroxypyrene-1,3,6-trisulfonate) by a short laser pulse, and the reprotonation of the pyranine anion was monitored at 457.8 nm. In parallel, the protonation of the membrane was followed at 496.5 nm, looking at the transient absorbance of fluorescein, covalently attached to the M side of the membrane. The analysis of the relaxation dynamics was carried out by a simulation procedure that reconstructs the observed dynamics of the two chromophores. The analysis revealed the presence of the membrane indigenous buffering moieties. The low-pK buffer (pK 4.1) was present in a quantity of 100 ± 20 nmol/mg of protein, and its kinetics indicate that it appears in multianionic clusters bearing a negative electric charge. The medium-pK buffer (pK 6.9) was present in a larger quantity (200 ± 20 nmol/mg), and its kinetic parameter indicated clustering into positively charged domains. Both types of indigenous buffer reacted with the proton and pyranine anion in unhindered diffusion-controlled reactions. On the other hand, the exchange of protons between the indigenous buffer moieties was rather slow. No evidence was found for the presence of sites capable of retaining a proton, secluded from the bulk, for a time frame longer than 100 μs as required by the models of localized proton gradient.

Since proton pumping was first described by Mitchell (1966), the mechanism of the reaction has been extensively investigated using steady-state measurements or rapid mixing systems [for review, see Mitchell (1976, 1987), Moody et al. (1987), Wikstrom et al. (1981), Woelders et al. (1981), and Papa (1989)].

The common methodology in these studies was to initiate a proton or electron flux by addition of substrate or (ATP) and to look for correlation between the ensuing fluxes (respiration, acidification, ion transport, or ATP synthesis). These measurments all share a common handicap, the mixing time of the system is orders of magnitude longer than the diffusion-controlled reaction of the proton. Up to the present, the elementary steps of proton interaction with the mitochondrial surface were not observed by any time-resolving measurement, and the kinetics had to be inferred from indirect enzymological experiments.

Some models for proton-coupled energy transformation (Nagle & Dilley, 1989; Sigalet et al., 1988; Guffanti & Krulwich, 1988; Ehrenheim et al., 1992) postulate a temporal and spatial confinement of the hydrated proton at some sites of the membranal coupling machinery. While these models were based on biochemical experiments, they must be supported by direct measurements of proton–membrane interactions.

In the present communcation, we describe the results of kinetic measurements monitoring the reversible binding of protons to the surface of native, tightly coupled submitochondrial vesicles. For that purpose the inside-out submitochondrial particles were covalently labeled with fluorescein and subjected to pulse protonation by discharging protons from a photoexcited dye, pyranine (8-hydroxypyrene-1,3,6-trisulfonate). The excited dye releases the hydroxyl proton with subnanosecond dynamics, and the proton diffuses in the solution, reacting in a diffusion-controlled reaction with any proton-binding moiety, the carboxylates (and other bases) on the membrane, the covalently bound fluorescein, and the ground-state anion (ΦO^-) of pyranine. In parallel with that reaction, the ΦO^- diffuses and obstructs a proton from any protonated compound with a pK lower than that of the dye. Thus the surface of the membrane is probed simultaneously by two particles, a positively charged proton and negatively charged anion (ΦO^-). The outcome of these two competing reactions determines the momentary state of protonation of each element on the membrane.

The observed signals were analyzed by a numerical integration of a set of differential rate equations which account, quantitatively, for all reactions proceeding in the perturbed space (Yam et al., 1988). By this procedure we determine for each component the rate constant of its reaction with H^+,ΦO^- and the rate of proton exchange among the surface groups.

The evaluation of the rate constants of each individual reaction is based on the equation of Debye–Smoluchowski for diffusion-controlled reactions between charged bodies. The carboxylates on the surface behaved as a negatively charged patch which attracts protons from the bulk and repels the ΦO^- anion ($Z = -4$). The basic moieties on the surface also behaved as clusters that repel the protons and attract the pyranine anions. Thus by looking at the kinetics of protonation of the membranal bound indicator, we could observe the microscopic structure of negative charged phospholipids and the positively charged proteins of the mitochondrial inner membrane.

The capacity to deduce the intimate structure around a target from time-resolved measurement may be further exploited using a more selective proton target on the mitochondrial surface.

† This research is supported by the Office of Naval Research of the U.S. Navy (N00014-89-J-1622).

* Author to whom correspondence should be addressed.

0006-2960/93/0432-2942$04.00/0

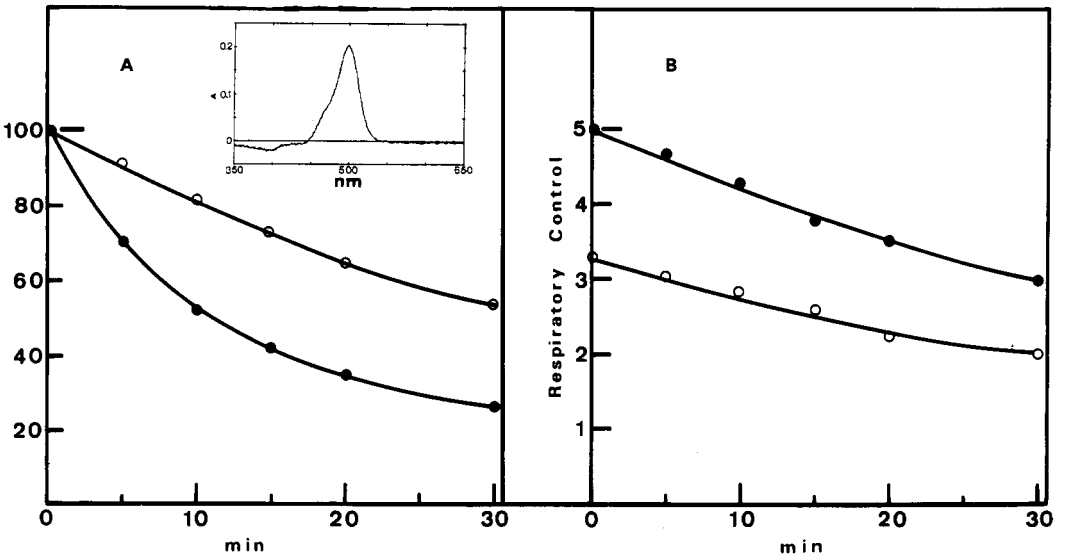

FIGURE 1: The inactivation of the catalytic activities of submitochondrial vesicles during labeling by fluorescein isothiocyanate. SMP (5 mg/mL) coupled by addition of oligomycin (0.5 μg/mg of protein) were suspended in 0.1 M HEPES and 0.2 mM EDTA (K-salts) at pH 9.2 and treated at 30 °C by 0.5 mM fluorescein isothiocyanate. Samples were taken at intervals and assayed for NADH oxidase (●) and succinoxidase (○) activities (see Materials and Methods). Panel A depicts the decline of oxidase activities. Panel B quantitates the decrease of the respiratory control ratio, measured as the acceleration of respiration upon addition of 2 μg/mL gramicidin. The uncoupled activities were 1.3 and 1.2 μmol/(min·mg) for NADH and succinate, respectively. (Insert) The difference spectrum of 0.12 mg/mL fluorescein labeled vesicles measured at pH 8.5 *minus* pH 6.7.

MATERIALS AND METHODS

Submitochondrial particles (SMP) used throughout this study were prepared essentially as described by Racker and Horstman (1967).

The binding of fluorescein isothiocyanate (FITC) to submitochondrial particles (5 mg/mL) was carried out when suspended in solution containing 0.5 mM FITC, 0.1 M HEPES, and 0.2 mM EDTA (K-salts), pH 9.2, at 30 °C. The labeling was terminated by a passage of the vesicles through a Sephadex G-50 (Course) column (20 × 1 cm) preequilibrated with 0.25 M sucrose adjusted to pH 8.5–8.6. The column also removes the buffers (HEPES, EDTA) from the medium as these compounds compete with the indicator for the protons released during the laser pulse (see below).

NADH oxidase activity of the SMP was measured at 30 °C at 340 nm in 0.25 M sucrose solution containing 1 mg/mL bovine serum albumin, 0.12 mM EDTA, and 20 mM HEPES, pH 8 (all K-salts), and 100 μM NADH. Succinoxidase was measured spectrophotometrically at 240 nm at 30 °C in the above solution, using 20 mM potassium succinate instead of NADH. The molar extinction coefficient of fumarate at 240 nm is 2.9×10^3 M^{-1} cm^{-1}.

Time-resolved measurement of proton transfer was carried out using the methodology detailed by Gutman (1984, 1986) and Yam et al. (1988). The photodissociation of protons from pyranine was initiated by a 3-ns (full width at half-maximum) pulse of the third harmonic frequency of Nd–Yag laser (λ = 355 nm) with energy density of 1 mW/cm^2 operating at 10 pps. The changes in protonation state of the fluorescein (λ = 496.5 nm) and pyranine anion (λ = 457.8 nm) were recorded by monitoring beams from a CW argon laser. Transient changes of the monitoring beam intensities were measured by a photomultiplier (rise time 15 ns) coupled to a Tektronix 2430 digital oscilloscope and averaged by an Olivettti 300 computer.

RESULTS

Binding of Fluorescein to SMP. The effect of FITC binding on the catalytic properties of submitochondrial vesicles is summarized in Figure 1. As seen in Figure 1A, both NADH oxidase and succinoxidase activities decline monotonically with time, where the former is somewhat more sensitive than the latter. The coupling of the vesicles, expressed as the respiratory control ratio (Figure 1B), also decreases with time. While the enzymic functionality decreases over a rather long period, the amount of dye bound to the membranes reaches a steady level of ~25 nmol/mg of protein within 10–15 min. A longer exposure of the vesicles to the labeling mixture hardly increases the amount of bound dye. For these reasons we terminated the labeling after 15 min.

The fluorescein bound to the membrane is readily detected by its absorption spectrum (insert to Figure 1A). At the pH range 6–8.5 the membrane-bound indicator followed a monotonic symmetric titration curve with inflection of pH 7.2 ± 0.05. The slope of the curve in the Henderson–Hasselbach plot (0.85) indicated some heterogeneity. For our calculations (see below) we assumed a single population with pK = 7.2.

Time-Resolved Kinetics of the Protonation of the Membrane-Bound Fluorescein. Submitochondrial vesicles labeled with fluorescein were suspended at 1 mg/mL in solution containing 0.25 M sucrose, 20 mM KCl, and 50 μM pyranine, pH 7.4. A volume of ~0.4 mL of the suspension was placed in a four-face quartz cuvette, and its content was constantly stirred by a magnetic disc. The sample was probed by a continuous beam of an argon laser either at 496.5 or 457.8 nm, which recorded the state of protonation of the fluorescein or the pyranine, respectively. The space probed by the argon laser beam was subjected to a series of short pulses of the third harmonic frequency of Nd–Yag laser. Each excitation pulse initiated a transient deprotonation of the pyranine, and the perturbed state of protonation of the two chromophores was recorded as it relaxed to the equilibrium level. The whole perturbation lasted ~100 μs. Thus the 100-ms interval between the excitation pulses is sufficiently long to allow the system to attain a full relaxation. The irradiation itself, either of the monitoring beam or the excitation pulses, caused no

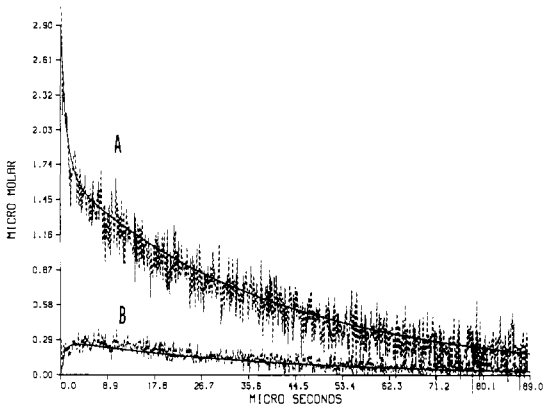

FIGURE 2: Time-resolved measurement of proton transfer between bulk and mitochondrial surface. The vesicles were suspended at 1 mg/mL in 0.25 M sucrose, 20 mM KCl, and 50 μM pyranine, pH 7.4, and exposed to 1024 repeating laser pulses of 2 mJ each. Curve A depicts the dynamics of reprotonation of pyranine anion monitored at 457.8 nm; curve B corresponds with the protonation of the membrane-bound fluorescein as measured at 496.5 nm. The continuous lines are the reconstructed dynamics [for details, see Gutman (1984, 1986)], using the parameters listed in Table I, column I.

damage to the catalytic activities of the preparation (data not shown).

Curve A in Figure 2 depicts the dynamics of the pyranine anion, the product of the proton dissociation from ΦOH^*. The formation of ΦO^- is too fast to be resolved, but its reprotonation is readily measured. The initial relaxation is fast, lasting 2–3 μs, followed by a slower phase. The prepulse concentrations are reached $\sim$100 μs after the initial perturbation.

Curve B describes the protonation of the membrane-bound indicator (R-Flu). There is a rapid rise in the concentration of the protonated indicator, which corresponds in time with the phase where ΦO^- undergoes rapid protonation (curve A), and then the indicator gradually loses its proton over a period comparable with the slow reprotonation phase of ΦO^-.

Curve A in Figure 2 quantitates the momentary concentration of the protons that were discharged from ΦOH, while those bound to the dye are given by curve B. The difference between the two corresponds with protons that are bound to the various carboxylates and amino moieties of the vesicles [the contribution of free protons to the balance is negligible (Gutman, 1984)]. We shall refer to these moieties as indigenous buffers and denote them as $R\text{-}NH_2$ and $R\text{-}COO^-$.

Figure 3A depicts the results of a similar experiment, except that the vesicles used for measurements were not labeled by FITC. In this preparation the only components reacting with the discharged protons are the indigenous buffer moieties, and their state of protonation is deduced from the reprotonation dynamics of ΦO^-. As seen in the figure, the reprotonation of ΦO^- commences at a fast rate, but after a few microseconds the reaction becomes rather slow, indicating that the protons discharged from ΦOH are retained by the indigenous buffer moieties on the native mitochondrial membrane.

Protonation of Disoriented Mitochondrial Membranes. The results described in Figures 2 and 3A were carried out with tightly coupled inside-out submitochondrial vesicles having a respiratory control ratio larger than 6 and correspond with proton binding to the matrix (M) side of the mitochondrial membrane.

At present, measurements of the proton binding dynamics to the cytosolic (C) side of the membrane are not experimentally feasible. Yet to satisfy our curiosity about the symmetry of the membrane, we looked at the protonation dynamics of a preparation that exposes both faces of the mitochondrial membrane to the bulk of the solution. This membrane preparation is collected by a long centrifugation of extensively sonicated mitochondria. This fraction exhibits slow rates of succinate or NADH oxidation but, on addition of cytochrome *c*, the respiration of both substrates is accelerated by 20-fold. In either case, the respiration rate is not accelerated by gramicidin. As cytochrome *c* and NADH interact with the membrane on opposite faces, the preparation represents disoriented vesicles. With this preparation we could monitor how the protons react with components present on the two sides of the mitochondrial membrane. The kinetics of pyranine reprotonation measured in the presence of disoriented membranes are shown in Figure 3B.

Analysis of the Experimental Observation. The analysis of the experiment is based on detailed reconstruction of all reactions proceeding in the perturbed sample through numerical integration of a set of nonlinear, coupled differential equations [for details see Gutman (1984, 1986) and Yam et al. (1988)]. In the present case, the following reactions were considered:

(A) Protonation of the pyranine and indigenous moieties by free diffusing protons (reactions 1–4).

$$H^+ + \Phi O^- \rightleftharpoons \Phi OH \quad (1)$$

$$H^+ + R\text{–}COO^- \rightleftharpoons R\text{-}COOH \quad (2)$$

$$H^+ + R\text{-}NH_2 \rightleftharpoons R\text{-}NH_3^+ \quad (3)$$

$$H^+ + R\text{-}Flu^- \rightleftharpoons R\text{-}FluH \quad (4)$$

(B) Proton exchange between ΦO^- and indigenous moieties.

$$\Phi O^- + R\text{-}COOH \rightleftharpoons \Phi OH + R\text{-}COO^- \quad (5)$$

$$\Phi O^- + R\text{-}NH_3^+ \rightleftharpoons \Phi OH + R\text{-}NH_2 \quad (6)$$

$$\Phi O^- + R\text{-}FluH \rightleftharpoons \Phi OH + R\text{-}Flu^- \quad (7)$$

(C) Proton exchange between indigenous moieties.

$$R\text{-}NH_2 + RCOOH \rightleftharpoons R\text{-}NH^+_3 + R\text{-}COO^- \quad (8)$$

$$R\text{-}Flu^- + R\text{-}COOH \rightleftharpoons R\text{-}FluH + R\text{-}COO^- \quad (9)$$

$$R\text{-}Flu^- + R\text{-}NH^+_3 \rightleftharpoons R\text{-}FluH + R\text{-}NH_2 \quad (10)$$

The equilibria were converted to differential rate equations, which were coupled according to the principle of detailed balance. The equations are listed in the appendix of Yam et al. (1988). The integration of the differential rate equations generates a dynamic curve that should reproduce the experimental observation. The precise reconstruction (see continuous curves in Figures 2, 3A, and 3B) was achieved by varying the magnitude of the rate constants and concentration of the indigenous buffer moieties as adjustable parameters. The experiments described in Figures 2 and 3 were repeated over a wide range of initial conditions, changing the prepulse pH and pyranine concentration. The experimental curves, collected for each preparation, were then analyzed. In this analysis, we obtained a single set of rate constants that reconstructs the dynamics of each preparation over the whole range of initial conditions (pH, pyranine, and vesicular concentrations of the reaction mixture). As documented in Table I, each preparation is characterized by one set of parameters which, for some reactions, differ markedly between the preparations. These rate constants are taken as characterizing the dynamics of bulk-surface proton transfer of the pertinent submitochondrial preparation.

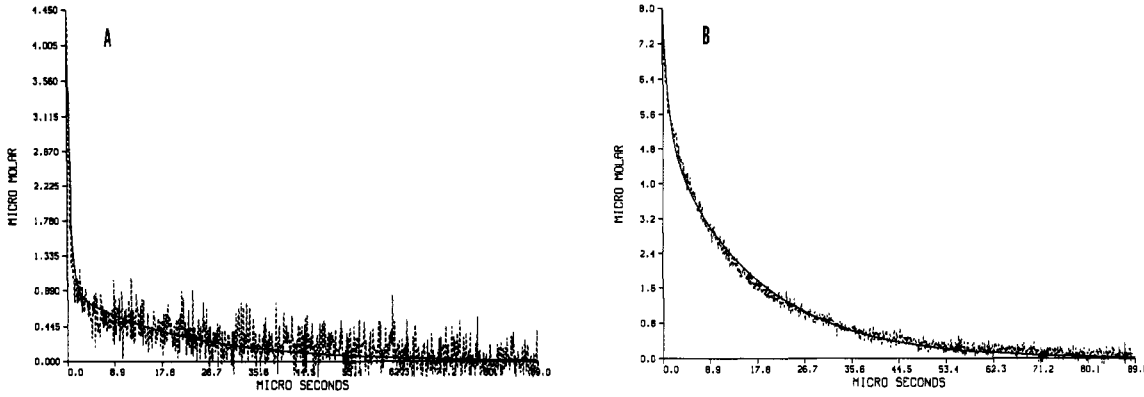

FIGURE 3: Time-resolved measurements of proton transfer between bulk and the surface of native submitochondrial vesicles. The reactions were measured as described in the legend to Figure 2, except that the vesicles were not treated by FITC. The observed signal is the reprotonation of the pyranine anion, generated by the laser pulse, measured at 457.8 nm. The continuous line is the reconstructed dynamics using the parameters given in Table I, columns II and III. (Panel A) 1 mg/mL native SMP in 0.25 M sucrose, 20 mM KCl, and 100 μM pyranine, pH 7.85. (Panel B) Unsealed fragments that were collected by a high-speed centrifugation (200000g for 180 min) of extensively sonicated heavy beef heart mitochondria. The fragments were suspended to 1 mg/mL in the sucrose KCl solution at pH 7.55 in the presence of 50 μM pyranine.

Table I: Stoichiometric and Kinetic Characteristics of the Reaction between Mitochondrial Membrane and Solvated Proton[a]

	preparation		
	FITC-SMP	SMP	unsealed fragments
1. pH of experiment	7.5	7–9	7–9
2. R-COO^- (nmol/mg)	110 ● 20	100 ± 10	130 ± 20
3. $pK_{(RCOOH)}$	4.1	4.1	4.1
4. R-NH_2 nmol/mg	180 ± 20	200 ± 20	200 ± 10
5. $pK_{(R\text{-}NH_3^+)}$	6.9	6.9	6.9
6. $\Phi O^- + H^+$	5×10^{10}	5×10^{10}	5×10^{10}
7. R-$Flu^- + H^+$	2.5×10^{10}		
8. R-$COO^- + H^+$	7×10^{10}	7×10^{10}	7×10^{10}
9. R-$NH_2 + H^+$	1×10^9	1×10^9	8×10^9
10. ΦO^- + R-COOH	5×10^7	5×10^7	5×10^7
11. ΦO^- + R-NH_3^+	1×10^7	4×10^8	4×10^8
12. ΦO^- + R-Flu H	1×10^9		
13. R-COOH + R-NH_2	1×10^9	3×10^9	1×10^9
14. R-COOH + R-Flu^-	1×10^{10}		
15. R-NH_3^+ + R-Flu^-	3×10^{10}		

[a] The values given in the table are the parameters which reconstruct the observed signals of the various preparations in the pH range listed on line 1. The rate constants are given in M^{-1} s^{-1} units, and their values are accurate within ±5%.

DISCUSSION

The Proton-Binding Capacity of the Mitochondrial Membrane. The results and analysis presented in this paper comprise the first systematic study of proton transfer dynamics between bulk phase water and a mitochondrial inner membrane preparation.

In the following discussion, we shall consider the nature of the indigenous proton-binding groups, evaluate the rate constants of their reactions, and draw conclusions about the structure of the membrane as "seen" by the proton.

The mitochondrial membrane bears a multitude of proton-binding sites, ranging from pK ~2 of the phospho moieties of each phospholipid (Nachliel & Gutman, 1988) up to pK ~12 of arginine. All of them are involved in the overall process of proton transfer between bulk and surface, but not to the same extent. A rigorous model that reconstructs the precise dynamics of the reaction should quantitate all reactants by their pK and concentrations, yet the larger the number of discrete components, the more complex are the computations. For this reason we omitted from our calculations the components of extreme pK values. This simplification is justifiable. The low-pK phosphomoieties retain a proton for only a few nanoseconds, an interval too short to affect dynamics lasting many tens of microseconds. The high-pK moieties like arginine, the ϵ-amino of lysines, and tyrosine are permanently protonated and are practically inert in our studies. Thus we include in the analysis only the medium-pK groups, i.e., carboxylates and pK ~7 amino moieties.

The quantitative representation of all indigenous buffers (carboxylates, histidins, and α-amino groups) was first tried by grouping them into one population with intermediate pK value. This simplification was too naive, and the computations failed to generate any acceptable reconstruction of the observed dynamics.

A more detailed model, where the carboxylates and medium-pK moieties were represented as two populations of unequal size, reproduced the dynamics with high fidelity. A more detailed model, having three, or more, types of indigenous buffer was of no analytic advantage. The amounts of indigenous buffers estimated for the three mitochondrial preparations are essentially the same. The low-pK population is identified to be mostly the acidic phospholipid headgroups (like phosphatidylserine). The medium-pK moieties represent the protein's surface. The amount of the reactive moieties corresponds to a buffer capacity at pH ~7.5 of 0.013 pH unit/10 μM H^+ at 1 mg/mL.

The Rate of Bulk–Surface Proton Transfer. The rate constant for the reaction of free protons with the indigenous groups on the membrane (lines 6–9 in Table I) falls within the acceptable range for diffusion-controlled reactions. Yet we find a 70-fold difference between the protonation rates of carboxylates and amino moieties (lines 8 and 9 in Table I), an observation that merits evaluation.

The study of Yam et al. (1991) on protonation dynamics of protein revealed that the rate constant of protonation of a chromophore is a reflection of the local charge, in its immediate vicinity, and not of the total charge carried by the protein. Thus by looking at the rate constants of specific moieties, we can gauge the local charge near the observed group, and if more than one moiety is studied, then the mosaic structure of charges on the membrane can be deduced. In the present study we applied this procedure for evaluating the mesoscopic organization of the indigenous buffer on the mitochondrial inner membrane.

The rate of protonation of the indigenous carboxylate anion was found to be faster than protonation of the free-diffusing pyranine anion ($Z = -4$) or the covalently bound double-

charged fluorescein anion (lines 6 and 7, Table I). An explanation for that phenomenon is based on the mesoscopic heterogeneity of electric charges on the mitochondrial membrane, over a length scale comparable with the dimension of a protein molecule. Within a negative charged domain, the rate constant of protonation of any anion is amplified by the charge of its neighbors. These negative domains are presumably the phospholipid matrix surrounding or interspaced between the proteins. A similar clustering of the positive charges (mostly probably on proteins) forms regions which repel the proton and lower the rate of their reaction with a free proton. Indeed, the rate of the R-NH_2 protonation is ~30% of that of a free-diffusing imidazol (Ophir and Gutman, unpublished results). Alternately, the slow rate may reveal the hindered accessibility of the $-NH_2$ moieties to the bulk.

Proton Transfer between Indigenous Buffer and a Free-Diffusing Molecule. The implication of charged domains as an explanation for the divergence in rate of protonatioin of the indigenous buffers is further corroborated by the rate constants of proton exchange between these buffers and the free-diffusing pyranine anion.

The carboxylate domains, which react rapidly with H^+, transfer their proton rather slowly to the $Z = -4$ pyranine anion, an indication for a strong repelling potential. The reaction of the amino moieties with the pyranine anion is much slower than a diffusion-controlled reaction. Such a slow process indicates their limited accessibility to large, bulky groups.

The binding of fluorescein to the membrane, mostly via lysine's ϵ-amino group, replaces the positive charge of the lysine by the negative charge of the chromophore. That treatment renders the protein region less positive. Indeed, we find that the amino moieties of fluorescein-labeled membranes react more slowly with ΦO^-.

Proton Transfer between the Indigenous Moieties. The proposed model, where the low- and high-pK moieties are segregrated into domains large enough to be kinetically distinguished, implies that the rate of proton exchange between domains will be relatively slow (see lines 13–15 in Table I).

The indigenous reactants cannot diffuse, one with respect to the other, and thus the rate of proton exchange among them is a function of their proximity. Close packing of sessile groups, with overlapping of Coulomb cages, will be revealed as high rates of reaction. In our previous studies we found that when donor and acceptor are close to each other, the rate of the reaction is about 10^{10} (Yam et al., 1988; Nachliel & Gutman, 1988). At a closer packing, as when both are located within an active site, the rate can be much faster, approaching the rate of intramolecular proton transfer [for review, see Shimoni et al. (1993) and Gutman and Nachliel (1990)]. The rates measured in the present work are substantially slower than 10^{10}, indicating that the mesoscopic domains are sufficiently large that the probability of proton transfer between them is slow. In contrast, the rates of R-COOH–fluorescein or RNH_3^+–fluorescein proton exchange are fast, indicating that the dye is accessible from both domains with comparable facility.

Anisotropy of Mitochondrial Membrane. The enzymes of the mitochondrial membrane exhibit functional anisotropy with respect to the surface of the membrane. The anisotropy can be indirectly inferred from the data given in Table I (columns II and III). The listed rate of reactions in both columns are identical except for the protonation of the amine component, which in the disoriented preparation is almost an order of magnitude faster than that of the M side face. Such a large difference implies that the charge distribution on the C and M sides are not identical. Extension of our present experiment to study selectively the protonation of the C side may reveal more features of the intricate structure of the mitochondrial membrane.

Concluding Remarks. Time-resolved proton-binding dynamics provide a new look at the buffering groups of the mitochondrial membrane. Detailed analysis of the observed signal reveals the rate constants of the reactions on the mitochondrial surface. Evaluation of these rate constants points to the presence of a heterogeneous surface made of positive and negative domains. The capacity to monitor experimentally the interaction between protons and the domains on the membrane may be a new step in the study of the detailed mechanism of energy transformation by respiring membranes.

REFERENCES

Ehrenheim, A. M., Vianelli, A., Finazzi, G., & Forti, G. (1992) *Biochim. Biophys. Acta 1100*, 299–302.

Guffanti, A. A., & Krulwich, T. A. (1988) *J. Biol. Chem. 263*, 14748–14752.

Gutman, M. (1984) *Methods Biochem. Anal. 30*, 1–103.

Gutman, M. (1986) *Methods Enzymol. 127*, 522–538.

Gutman, M., & Nachliel, E. (1990) *Biochim. Biophys. Acta 1015*, 391–414.

Mitchell, P. (1976) *J. Theor. Biol. 62*, 327–367.

Mitchell, P. (1986) *Chemiosmotic Coupling in Oxidative and Photosynthetic Phosphorylation*, Glynn Research, Bodmin, U.K.

Mitchell, P. (1987) *FEBS Lett. 222*, 235–245.

Moody, A. J., Mitchell, R., West, I. C., & Mitchell, P. (1987) *Biochim. Biophys. Acta 894*, 209–227.

Nachliel, E., & Gutman, M. (1988) *J. Am. Chem. Soc. 110*, 2629–2635.

Nagle, J. F., & Dielley, R. A. (1986) *J. Bioenerg. Biomembr. 18*, 55–64.

Papa, S. (1989) *Highlights Mod. Biochem. 1*, 781–796.

Racker, E., & Horstman, L. (1987) *J. Biol. Chem. 242*, 2547–2556.

Shimoni, E., Nachliel, E., & Gutman, M. (1993) *Biophys. J.* (in press).

Sigalat, C., de Kouchkowski, Y., Haraux, Z., & de Kouchkowsky, F. (1988) *Biochim. Biophys. Acta 934*, 375–388.

Theg, S. M., Chiang, G., & Dilley, R. A. (1988) *J. Biol. Chem. 263*, 673–681.

Wikstrom, M., Krab, K., & Saraste, M. (1981) *Annu. Rev. Biochem. 50*, 623–655.

Woelders, H., van der Velden, T., & van Dam, K. (1988) *Biochim. Biophys. Acta 934*, 123–134.

Yam, R., Nachliel, E., & Gutman, M. (1988) *J. Am. Chem. Soc. 110*, 2636–2640.

Yam, R., Nachliel, E., Kiryati, S., Gutman, M., & Huppert, D. (1991) *Biophys. J. 59*, 4–11.